Pure & Appl. Chem., Vol. 59, No. 10, pp. 1237–1246, 1987.
Printed in Great Britain.

Generation of coherent and tunable ultraviolet radiation by scattering processes

B. P. Stoicheff

Department of Physics, University of Toronto, Toronto, Ontario M5S 1A7, Canada

Abstract - Tunable, coherent radiation in the ultraviolet region has been generated by stimulated Raman scattering, by anti-Stokes Raman lasers, and by frequency-mixing processes based on nonlinear polarizabilities of atomic and molecular systems. Present progress in the development of these laser-driven sources is reviewed, with examples of available systems and their characteristics. Applications in spectroscopy are briefly discussed.

INTRODUCTION

Today, it is clear that laser sources have led to a complete revival of Raman spectroscopy with many important applications in physics, chemistry, and biology. And generally, the availability of tunable lasers in the visible and infrared wavelength regions has made possible significant advances in our understanding of the interaction of radiation and matter. At the present time there is a lack of lasers and especially of tunable lasers in the ultraviolet (UV), vacuum ultraviolet (VUV, from 200 to 100 nm), and extreme ultraviolet (XUV, from 100 to ~20 nm) regions of the spectrum. In fact, only a few lasers have been made to operate at these short wavelengths, in spite of considerable efforts being made in the past decade. The excimer lasers, such as XeF (315 nm), XeCl (308 nm), KrF (248 nm), ArF (193 nm), Xe_2 (~170 nm), and Ar_2 (~120 nm), and the H_2 laser (~110 nm) have been available for some time now, but these emit at discrete wavelengths or are tunable only over their relatively narrow bandwidths.

The difficulty in producing stimulated emission in the ultraviolet regions is well known, and arises from the basic relation that the probability for spontaneous emission, A, varies as $\nu^3 B$, where B is the probability for stimulated emission. Thus, losses in excited state population due to spontaneous emission increase rapidly at short wavelengths, and put severe demands on pumping sources in order to achieve inverted population. Various techniques are being explored to overcome these difficulties including recombination processes and excitation of ions; and in principle, the free-electron laser could operate at these short wavelengths. Much effort in this direction is being made in many laboratories, and we hope that new VUV and XUV lasers will soon be reported.

In the meantime, there has been substantial progress in producing VUV and XUV radiation by Raman scattering processes, by harmonic generation, and by frequency mixing of laser radiation in nonlinear media. The resulting radiation is coherent, monochromatic, directional, and tunable over broad regions, and thus has all the characteristics of laser radiation except for high intensity. Nevertheless, the intensities achieved to date are sufficient for many applications in absorption and fluorescence spectroscopy, and we can expect that excitation of Raman and Brillouin spectra will soon follow.

It is my purpose to review these accomplishments, to sketch the basic theoretical concepts, describe the experimental methods used in generating tunable, coherent VUV and XUV radiation, and to briefly discuss some recent spectroscopic applications.

STIMULATED RAMAN SCATTERING

Since the first observations of stimulated Raman scattering (ref. 1), it was clear that this process could be used to generate coherent radiation at prescribed wavelengths (ref. 2) by selection of the pump laser and Raman medium. In the intervening years, laser-stimulated Raman Stokes and anti-Stokes radiation has been produced at specific wavelengths in the infrared, visible, and extending into the vacuum ultraviolet region. It is of interest to note that some of the earliest experiments were carried out with liquids (ref. 2) N_2, O_2, and H_2, and with gases (ref. 3) H_2, D_2, and CH_4. These are the most efficient Raman scattering media, and today, the gases H_2, CH_4, and N_2 are the most generally useful for Raman shifting into the ultraviolet regions.

There are several comprehensive reviews (ref. 4) of theories of stimulated Raman processes and of salient experiments. For our purpose, we need only consider that when intense laser radiation (at frequency ω_0) is incident on a Raman-active medium, there is exponential growth of the spontaneous Stokes wave (at frequency ω_s) given by

$$I_s(1) = I_s(0)e^{gl}, \quad \text{with the gain} \quad g = (N_a - N_b)\left(\frac{d\alpha}{dq}\right)\frac{4\pi^2\omega_s}{n_0 n_s \mu \omega_0 \Gamma} \qquad (1)$$

Here, N_a and N_b are populations in the lower and upper states of the Raman transition, $d\alpha/dq$ is the rate of change of polarizability with normal coordinate, n_0 and n_s are the refractive indices at ω_0 and ω_s, Γ is the Raman linewidth and μ the reduced mass. Eq. (1) describes a Stokes Raman laser producing coherent radiation at ω_s. In this brief and simplified description, we may consider that the strong pump and Stokes waves generate a coherent material excitation at ω_r. This oscillation causes variations in the refractive index which then modulate and scatter the incident laser radiation (ω_0) thus producing sidebands or many orders of coherent Stokes and anti-Stokes radiation at frequencies $\omega_0 \mp n\omega_r$.

From Eq. (1) it is apparent that in molecular media, totally symmetric modes of vibration would lead to the highest Raman gain. This follows from our knowledge that in spontaneous Raman scattering these vibrational modes exhibit the largest rates of change of polarizability and the sharpest Raman lines. Also, since usually $N_a - N_b > 0$, an inverted population is not required for a Stokes Raman laser or for coherent anti-Stokes scattering. However, if $N_a < N_b$, then one has the possibility of an anti-Stokes Raman laser, with exponential gain at a higher frequency ($\omega_a = \omega_0 + \omega_r$) than that of the pump. Both anti-Stokes coherent Raman scattering and anti-Stokes Raman lasers now provide UV and VUV radiation. Recent progress will be reviewed below.

Anti-Stokes Raman scattering

While the earliest anti-Stokes (AS) Raman shifting experiments with H_2, CH_4, and N_2 were carried out with ruby laser excitation (refs. 2,3), any significant progress in reaching the far UV and VUV regions was only achieved with the availability of excimer laser radiation in the late 70's. Initially several orders of stimulated Stokes emission and one or two orders of anti-Stokes emission were generated with KrF (248 nm) and ArF (193 nm) excitation (ref. 5). However, up to 5 AS lines were observed (ref. 6) with pressurized H_2 ($\Delta\nu$ = 4155 cm^{-1}) and ArF excitation, with the shortest wavelength being 138 nm. In another experiment tunable dye laser radiation (ref. 7) (Rh 101 dye and 9 ns pulses) of 30 mJ energy provided 9 AS components of H_2 to reach 185 nm. This was extended to the 13th AS line to generate VUV radiation at 138.5 nm (Fig. 1) using the experimental arrangement (ref. 8) shown in Fig. 2. A Nd:YAG laser was used to generate ~300 mJ of second harmonic radiation at 532 nm, and this in turn pumped a dye oscillator-amplifier system to emit ~100 mJ at 545 nm. This radiation was focussed in a one meter Raman cell of H_2 at a pressure of 2-3 atm, to yield up to 13 AS lines. The emitted energy was detected and measured with an evacuated prism spectrometer. In a more recent modification of this experiment, Döbele et al. (ref. 9) amplified the radiation of the 8th H_2 AS component at 193 nm in three ArF amplifiers and used the output (~40 mJ) to excite up to the 6th H_2 AS component at 130 nm. Under these circumstances high power pulses (~0.8 kW) of a few nanosecond duration were obtained at 130 nm.

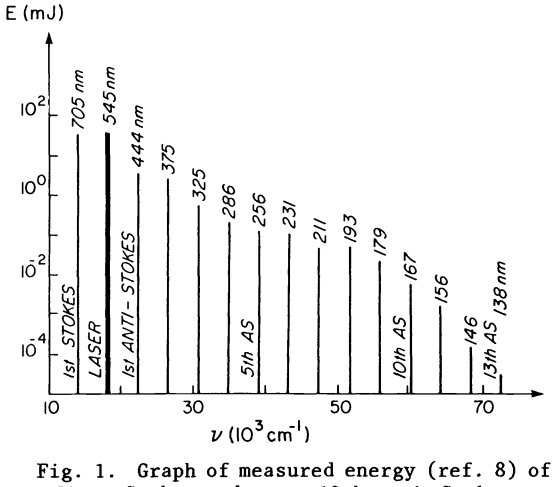

Fig. 1. Graph of measured energy (ref. 8) of first-Stokes and up to 13th anti-Stokes emission in H_2 gas at a pressure of 5 atm excited by laser radiation at 545 nm with the experimental arrangement shown in Fig. 2.

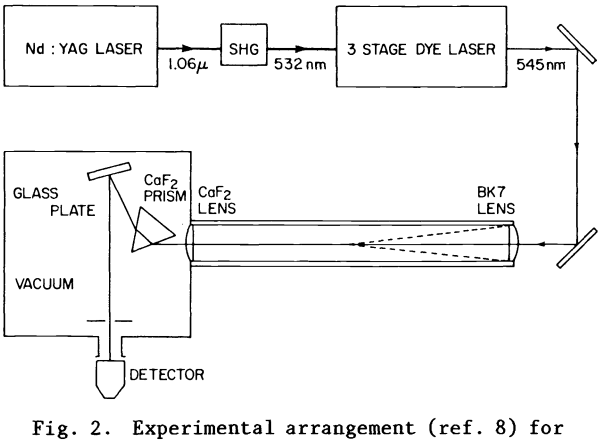

Fig. 2. Experimental arrangement (ref. 8) for generating many orders of anti-Stokes coherent emission in H_2 gas.

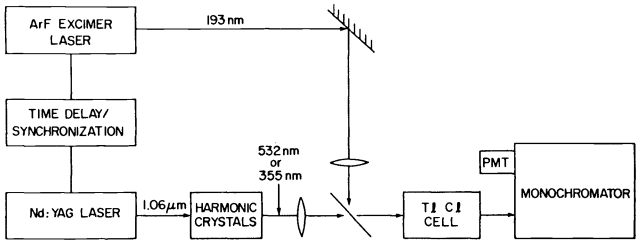

Fig. 3. Experimental arrangement used to produce a Thallium anti-Stokes Raman laser (ref. 14).

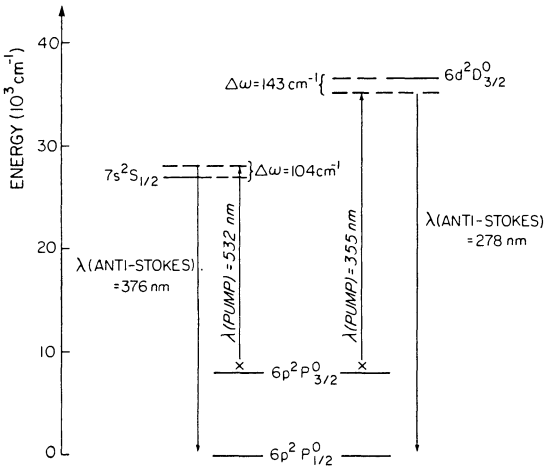

Fig. 4. Energy levels involved in the Thallium anti-Stokes Raman laser (ref. 14) with inverted population in the $6p^2P_{3/2}$ level and pump sources at 532 and 355 nm.

Recently, a XeCl laser (308 nm) with high spectral brightness has been used by Maeda and Takahashi (ref. 10) to excite up to the 11th AS component at 128.3 nm in H_2 gas at 10 atm. This source and therefore the AS Raman emission is tunable over the bandwidth of the XeCl laser (~10Å). The potential for emission at much shorter wavelengths now exists with excitation of stimulated Raman scattering with an E-beam pumped Ar_2 excimer laser operating at 124 to 127.5 nm with ~2 MW output power. In preliminary experiments, Sasaki et al. (ref. 11) have generated ~100 kW power in the first and second order Stokes emission (at 134 and 141 nm) of H_2 at 8 atm pressure, and are pursuing their investigation in the anti-Stokes region.

Anti-Stokes Raman lasers

As already mentioned above, when a population inversion exists between the upper and lower Raman levels, that is when $N_b > N_a$ in Eq. (1), stimulated anti-Stokes emission may be induced at a wavelength shorter than that of the pump laser. Such an anti-Stokes Raman laser would in principle yield high output energy since the upper Raman level is usually metastable, and moreover would be tunable by tuning the pump laser.

In the earliest experiments (ref. 12), gain was measured in the anti-Stokes signal when the excited $^2P_{1/2}$ state of I* was inverted relative to the $^2P_{3/2}$ ground state by flash photolysis of CF_3I, and then pumped by 1.06 μm radiation from a Nd:YAG laser. In 1977, Harris and coworkers (ref. 13) proposed and demonstrated a bright and tunable XUV source based on spontaneous anti-Stokes scattering from an atomic population stored in the $2s^1S$ metastable level of He (at ν = 166272 cm^{-1}). In their experiments, pulsed laser radiation at 1.06 μm (ν_p ~ 9395 cm^{-1}) was focused in the He discharge; and spontaneously emitted radiation at $\nu_p + \nu_p$ (56.9 and 63.7 nm) was observed at right angles to the incident pump beam. This radiation exhibited several unique properties: linear polarization, narrow linewidth (~1 cm^{-1} compared to 5.6 cm^{-1} of the He resonance line in the discharge) and high peak spectral brightness (~100 times brighter than the resonance line). Tunability over a range of ~60,000 cm^{-1} in the vicinity of 58 nm could be achieved by pumping atoms out of the metastable state with tunable dye laser radiation.

The first anti-Stokes Raman laser was reported in 1982 by White and Henderson (ref. 14). Thallium vapor was used as the Raman medium with inversion of the $6p^2P_{3/2}$ level relative to the $6p^2P_{1/2}$ ground level produced by selective photodissociation of TlCl by 193 nm radiation from an ArF laser. With the second and third harmonics (at 532 and 355 nm, respectively) of a Nd:YAG laser as pump sources, anti-Stokes laser emission was observed at 376 and 278 nm, respectively. The experimental arrangement and relevant energy levels are shown in Figs. 3 and 4.

In a series of papers on various anti-Stokes laser media, White and Henderson (ref. 14) demonstrated such laser emission at 178 nm from I, at 149 nm from Br, and 410 nm from In. White (ref. 15) also proposed that anti-Stokes lasers with emission from 100 to 206 nm could be produced based on metastable population inversions in the group VI elements O, S, Se from selective photodissociation of N_2O, OCS, and OCSe by VUV radiation. In recent experiments, Ludewigt et al. (ref. 16) have achieved anti-Stokes Raman-laser emission in Se at 158.7 and 167.5 nm using pump-laser radiation at 199.5 and 254.8 nm, respectively. Anti-Stokes Raman lasers using Sn and Pb have also been reported (ref. 17).

HARMONIC GENERATION AND FREQUENCY MIXING

Theory

Laser-driven VUV sources are based on third harmonic generation (THG) or 4-wave sum mixing (4-WSM) in nonlinear media. These processes are usually described by the induced macroscopic polarization of the medium which, of course, is dependent on the polarizabilities of the atomic or molecular systems when irradiated by intense laser light (Armstrong et al. (ref. 18)). It is well known that the polarization of a medium in the presence of a monochromatic field $\bar{E}(r,t) = \Sigma_i E(\omega_i)$ can be written as

$$\bar{P}(\omega_i) = \chi^{(1)}(\omega_i) \cdot \bar{E}(\omega_i) + \Sigma\chi^{(2)}(\omega_i = \omega_j + \omega_k) \cdot \bar{E}(\omega_j) \cdot \bar{E}(\omega_k)$$

$$+ \Sigma\chi^{(3)}(\omega_i = \omega_j + \omega_k + \omega_\ell) \cdot \bar{E}(\omega_j) \cdot \bar{E}(\omega_k) \cdot \bar{E}(\omega_\ell) + \ldots .$$

where $\chi^{(n)}$ are the susceptibility tensors of nth order. The lowest order term producing nonlinear effects is $\chi^{(2)}$. However, this tensor has nonzero components only in noncentro-symmetric systems: isotropic media such as cubic crystals, liquids, and gases do not exhibit quadratic nonlinearities. For third order processes such as THG and 4-WSM we need be concerned only with $\chi^{(3)}$, whose principal term may be written

$$\chi^{(3)}(\omega_0 = \omega_1 + \omega_2 + \omega_3) = \frac{3e^4}{4\hbar^3} \frac{\langle g|\mu|a\rangle\langle a|\mu|b\rangle\langle b|\mu|c\rangle\langle c|\mu|g\rangle}{(\Omega_{cg} - \omega_1 - \omega_2 - \omega_3)(\Omega_{bg} - \omega_1 - \omega_2)(\Omega_{ag} - \omega_1)} \qquad (2)$$

Here, $\langle g|\mu|a\rangle$ is the electric dipole matrix element between the ground state $|g\rangle$ and an excited state $|a\rangle$, having a lifetime Γ_a, and $\Omega_{ag} = \omega_{ag} - i\Gamma_a/2$ is the energy difference (Fig. 5) between states $|a\rangle$ and $|g\rangle$, e is the electronic charge and $\hbar = h/2\pi$, with h being Planck's constant.

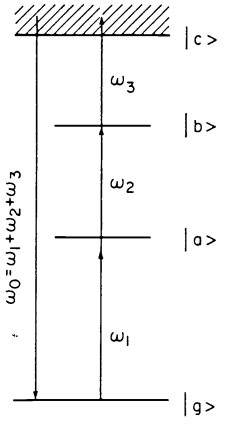

Fig. 5. Schematic energy level diagram based on Eq. (2) and illustrating the four-wave sum-mixing (4-WSM) process $\omega_0 = \omega_1 + \omega_2 + \omega_3$ with a 2-photon resonance ($\Omega_{bg} - \omega_1 - \omega_2 = 0$).

Equation (1) shows that $\chi^{(3)}$ will be resonantly enhanced whenever the applied frequencies, ω_1, ω_2, ω_3, are such that the real part of the resonance denominator vanishes, namely when $(\Omega_{ag} - \omega_1) = 0$, or $(\Omega_{bg} - \omega_1 - \omega_2) = 0$, or $(\Omega_{cg} - \omega_1 - \omega_2 - \omega_3) = 0$, corresponding to one, two, or three photon resonance, respectively. If any of ω_1, ω_2, ω_3 is set equal to a resonance frequency (Ω_{ag} etc.), $\chi^{(3)}$ will be enhanced but the incident radiation will be strongly absorbed. Similarly if $\omega_0 = \omega_1 + \omega_2 + \omega_3$ equals a resonance frequency, the generated radiation will be absorbed. If however, $\omega_1 + \omega_2$ is equal to a 2-photon resonance (Ω_{bg}), the incident radiation at $\omega_1 + \omega_2$ is expected to be only weakly absorbed by the 2-photon transition, while the resonance enhancement of $\chi^{(3)}$ could be just as strong as for the 1-photon resonances.

For third harmonic generation (THG), $\chi^{(3)}$ simplifies to

$$\chi^{(3)}(\omega_0 = 3\omega) = \frac{3e^4}{4\hbar^3} \frac{\langle g|\mu|a\rangle \text{ etc.}}{(\Omega_{cg} - 3\omega)(\Omega_{bg} - 2\omega)(\Omega_{ag} - \omega)} \qquad (3)$$

When 2ω approaches resonance, $\chi^{(3)}$ undergoes strong ($>10^4$) enhancement. For efficient THG, collinear phase-matching is necessary, that is, the refractive index $n(3\omega) = n(\omega)$ in order to yield a maximum effective interaction length. With focused incident radiation, THG can be observed only in negatively dispersive media. Tunability is achieved by varying the incident frequency ω.

For generating tunable radiation by 4-WSM, the process $\omega_0 = 2\omega_1 + \omega_2$ is of interest. $\chi^{(3)}$ then becomes

$$\chi^{(3)}(\omega_0 = 2\omega_1 + \omega_2) = \frac{3e^4}{4\hbar^3} \frac{\langle g|\mu|a\rangle \text{ etc.}}{(\Omega_{cg} - 2\omega_1 - \omega_2)(\Omega_{bg} - 2\omega_1)(\Omega_{ag} - \omega_1)} \quad (4)$$

Strong enhancement is again achieved by tuning $2\omega_1$ to a parity-allowed 2-photon resonance, Ω_{bg}. Tunability (and further enhancement) is then obtained by selecting ω_2 so that $2\omega_1 + \omega_2$ corresponds to the ionization continuum or to broad autoionizing levels above the ionization limit (Hodgson et al. (ref. 19)). More detailed treatments of the relevant theory including phase-matching, saturation effects, and conversion efficiencies have been given by Vidal (ref. 20) and Jamroz and Stoicheff (ref. 21).

Experimental techniques

Obviously, any medium used for generating radiation at wavelengths below 200 nm must be transparent to such radiation. This condition is generally met by the rare gases and some metal vapors. New and Ward (ref. 22) were the first to demonstrate THG in gases. Subsequently, Harris and Miles (ref. 23) showed that relatively high conversion efficiency of THG and 4-WSM could be obtained by using phase-matched metal vapors as nonlinear media, and that efficiency could be improved further by resonance enhancement.

Frequency conversion into the VUV and XUV regions has been achieved by a variety of laser systems. Powerful pulsed lasers such as ruby, Nd:YAG, Nd in glass, flashlamp pumped dye (FPD), rare gas excimer, and rare gas halide exciplex lasers provide the primary coherent radiation. In some systems, tunable radiation from dye lasers (> 320 nm) is used directly, and in others laser radiation (> 400 nm) is doubled once or twice in nonlinear crystals to produce coherent radiation in the UV to about 200 nm. Subsequently, the coherent UV radiation is converted to coherent VUV and XUV by THG or frequency mixing in rare gases or metal vapors. These methods all use a cell or heat pipe to contain the nonlinear gas. Windows of LiF are used to the limit of transmittance at ~104 nm; for generation to shorter wavelengths, pinholes (ref. 24) and capillary arrays (ref. 25) with differential pumping are used. Recently, pulsed supersonic jets have been introduced for harmonic generation with rare gases (refs. 26,27). Specific atomic (and molecular) systems are selected because of their large third order nonlinear susceptibility, suitability of energy levels for resonance enhancement, and low absorption at the desired VUV or XUV wavelength.

In our laboratory, we use essentially the same 4-WSM technique as that described by Hodgson, Sorokin, and Wynne (ref. 19) who generated VUV radiation tunable from 200 to 177 nm in Sr vapor. By using Mg, Zn, or Hg (ref. 28) vapor as the nonlinear medium, we have extended the tuning range to the transmission limit of LiF windows at ~104 nm. The experimental arrangement is shown in Fig. 6. A N_2 laser (Molectron-UV1000) or excimer KrF/XeCl laser (Lumonics TE-861M) pumps two dye lasers at frequencies ν_1 and ν_2. With the N_2 laser pump, each dye laser produces ~10 kW pulses of ~7 ns duration with linewidths ~0.1 cm^{-1}. Resonance enhancement of $\chi^{(3)}$ is achieved by setting $2\nu_1$ to a 2-photon resonance in the atomic system, and the second laser (ν_2) is scanned over the breadth of a suitable autoionizing level to obtain a broad range of tunability (Fig. 7). The two beams are spatially overlapped in a Glan-Thompson prism, and focused near the exit end of a heat-pipe

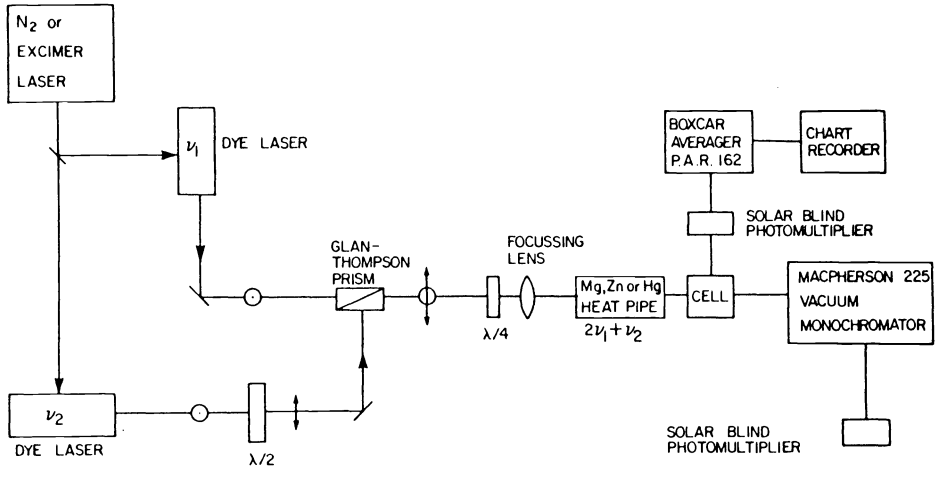

Fig. 6. Method of exciting two tunable dye lasers and of combining radiation at ν_1 and ν_2 to generate tunable coherent VUV radiation by 4-WSM in a metal vapor (refs. 19,28).

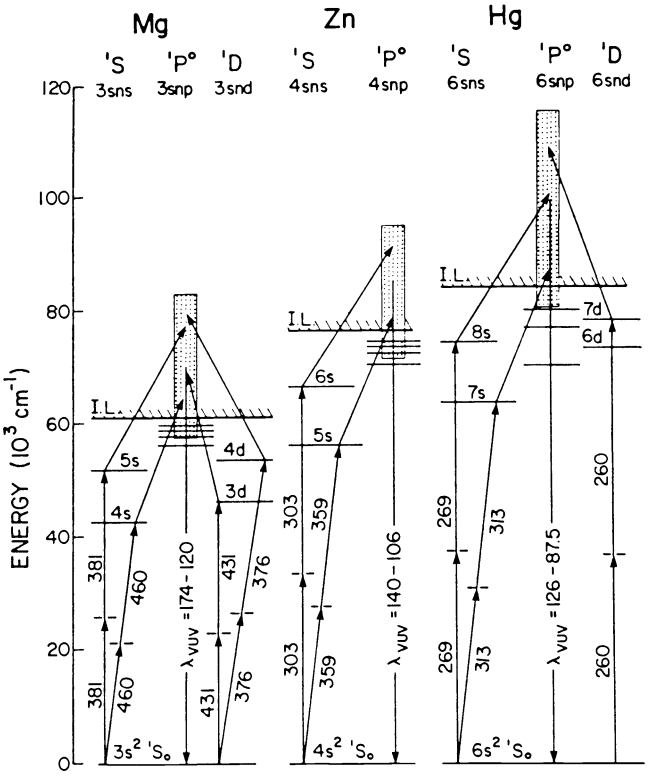

Fig. 7. Partial energy-level diagrams for atomic Mg, Zn, and Hg. Levels used for 2-photon resonance enhancement of 4-WSM are shown (along with necessary wavelengths in nanometers). The regions of ionization continua and broad autoionizing levels that contribute to the tunability of these sources are indicated by the hatched areas (refs. 25,28).

containing Mg vapor at ∿200 torr. The resulting coherent radiation is continuously tunable from 174 to 135 nm with a flux $>10^8$ photons per pulse. For generating shorter wavlength radiation, the excimer laser is used to pump two dye laser oscillator-amplifier systems with outputs of ∿50 kW. One of the beams is frequency-doubled in a KDP crystal to produce the 2-photon resonance enhancement, $2\nu_1$, of a suitable level in Mg, Zn or Hg vapor. With Zn vapor, a flux of $\sim 10^7$ photons per pulse is generated from 140 to 106 nm, and with Hg vapor an increase of 10^2 to 10^3 in flux is achieved over the tuning range of 120 to 104 nm, but decreases rapidly on going to 87.5 nm (ref. 25).

The early work of Harris and coworkers (ref. 29) on nonlinear mixing in Xe and Ar was followed by work on Kr and Xe. Extensive wavelength tunability with rare gases was reported by Hilbig and Wallenstein (ref. 30). They used sum-frequency mixing ($\omega_{VUV} = 2\omega_{UV} + \omega_D$) in Kr and Xe to generate VUV radiation of ∿20 W power, tunable over most of the range 110 to 130 nm where these gases are negatively dispersive. They also generated VUV radiation of ∿50 W power at longer wavelengths in Xe by difference-frequency mixing. The process $\omega_{VUV} = 2\omega_{UV} - \omega_D$ resulted in radiation from 185 to 207 nm, and $\omega_{VUV} = 2\omega_{UV} - \omega_L$ at shorter wavelengths, from 160 to 190 nm. (The frequencies ω_L, ω_D, and ω_{UV} refer to the output of a Nd:YAG laser, a dye laser and harmonic of the dye laser, respectively.) For these experiments, Hilbig and Wallenstein used the second harmonic radiation of a Nd:YAG laser (λ_L) to excite a dye-laser oscillator-amplifier system. This system operated at λ_D = 550 to 650 nm, with output powers of 3 to 5 MW in pulses of ∿6 ns duration, and with a bandwidth of ∿0.02 cm^{-1}. This tunable visible radiation was then doubled in KDP to produce tunable UV radiation (λ_{UV}) at powers of ∿1 MW. Both visible and ultraviolet radiation was focused in the rare gas, and the resulting VUV radiation analyzed with a monochromator and detected by a solar-blind photomultiplier and NO ionization cell. This multi-laser system, with further flexibility in order to fill in the few gaps in tuning range, will be a useful source for spectroscopy in the region 100 to 200 nm. More recently Wallenstein and his group have generated XUV radiation by nonresonant frequency tripling in Ar (from 97.4 - 104.8 nm) and in Ne (in the region 72-74.4 nm) (ref. 31).

Higher order frequency conversion has been used to generate radiation at fixed frequencies to wavelengths as short as 38 and 35.5 nm. Reintjes et al. (ref. 32) have used the fundamental, second, and fourth harmonics of a mode-locked Nd:YAG laser to generate XUV

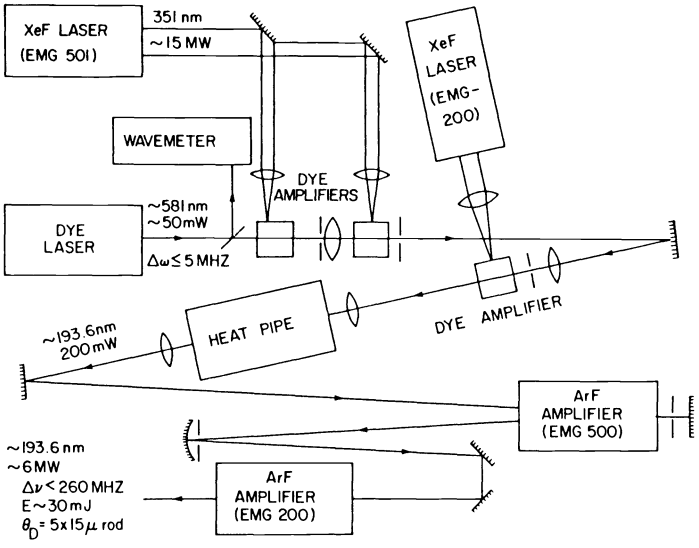

Fig. 8.
A high spectral brightness laser system (ref. 33) used in generating VUV radiation.

radiation in rare gases in third through fifth and seventh harmonic conversion. Fifth harmonic of 266.1 nm radiation produced radiation at 53.2 nm in He, Ne, Ar and Kr, with peak pulse powers of ∿1 kW in He. Seventh harmonic at 38 nm was observed in He with peak power of ∿100 W. Recently, Bokor et al. (ref. 26) have used a supersonic He gas jet to produce radiation at 35.5 nm by seventh-harmonic conversion of 248 nm radiation from a KrF excimer laser.

Rhodes and his colleagues (ref. 33) have developed KrF and ArF laser systems of extremely high brightness for use in THG and 4-WSM below 100 nm. A schematic outline of a typical multi-laser system is shown in Fig. 8. The tunable output of a single-frequency, cw dye laser at ∿580 nm was pulse-amplified in a three-stage, XeF-pumped, amplifier. The ∿10 ns, 20 mJ pulses were focused into Sr vapor to generate third harmonic radiation at ∿193 nm, in 5 ns pulses of 200 mW peak power. These pulses were then amplified in two ArF laser amplifiers to produce ∿5 ns pulses of 6 MW peak power and ∿0.01 cm^{-1} bandwidth, tunable within the ArF gain profile. This radiation was focused and tripled to 64 nm in Kr, Ar, and H_2. Another similar system with a final KrF amplifier generated radiation at 248 nm. This was tripled in flowing Xe to produce radiation at ∿83 nm.

In Fig. 9 is shown the system developed by Kung and his colleagues (refs. 27,36) for use with gases at high densities, emitted from a pulsed supersonic nozzle, as nonlinear media. The pump source of Nd:YAG - dye laser - and frequency doubler provided tunable radiation of ∿10 MW at ∿300 nm, for frequency tripling in Xe, Kr, Ar, Ne, H_2 or CO. Ar was the most efficient, giving ∿10^8 photons per 3 ns pulse (and 10W peak power) over the range 102.3 to 97.3 nm.

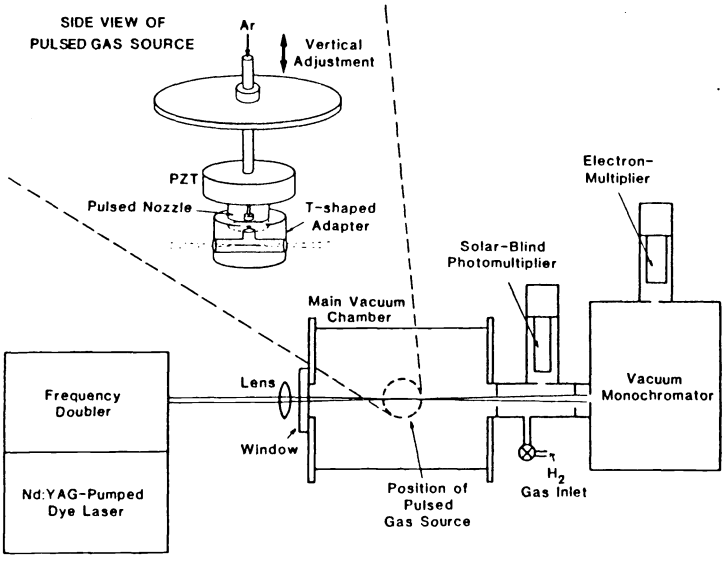

Fig. 9.
Laser and pulsed supersonic jet (refs. 27,36) with Xe, Kr, Ar, Ne, H_2 or CO used to produce VUV and XUV radiation by third harmonic generation.

TABLE 1. Tunable Generation in Rare Gases

λ(nm)	Nonlinear Medium	Processes	Primary Laser	Reference
206 - 160[a]	Xe	$2\lambda_{UV} - \lambda_L$	Nd:YAG-Dye	30
195 - 163	Xe	$2\times266\pm\lambda_s,\lambda_i$[b]	Nd:YAG and PO[b]	29
147 - 118	Xe	$2\times266\pm\lambda_s,\lambda_i$[b]	Nd:YAG and PO[b]	29
147 - 140	Xe:Kr	$3\lambda_{Dye}$	Nd:YAG-Dye	30
130 - 110[a]	Kr	$2\lambda_{UV}+\lambda_L$	Nd:YAG-Dye	30
123.6-120.3	Kr	$3\lambda_{Dye}$	KrF-Dye	34
123.5-120	Kr:Ar	$3\lambda_{Dye}$	Nd:YAG-Dye	30
106.8-105.8	Xe	$3\lambda_{Dye}$	Nd:YAG-Dye	35
102.3-97.3	Ar	$3\lambda_{Dye}$	Nd:YAG-Dye	36,31
73.6-72.0	Ne	$3\lambda_{Dye}$	Nd:YAG-Dye	31

[a] λ_{UV} from a range of laser dyes.
[b] PO ≡ parametric oscillator (signal and idler wavelengths λ_s,λ_i).

TABLE 2. Tunable Generation in Metal Vapors

Nonlinear Medium (Ioniz. Limit, nm)	λ(nm)	Primary Laser	Reference
Sr(217.8)	195.7-177.8	N_2-Dye	19
Mg(162.1)	174 - 130	N_2-Dye	28
	129 - 120	KrF-Dye	28
Zn(132.0)	140 - 106	XeCl/KrF-Dye	28
Hg(118.0)	125.1-117.4	Nd:YAG-Dye	37
	115.0-93.0	Nd:YAG-Dye	38
	196 - 109	Nd:YAG-Dye	31
	126 - 87.5	XeCl-Dye	25,28

The nonlinear media and laser systems used at the present time to generate tunable, coherent, VUV and XUV radiation are summarized in Tables 1 and 2, along with their regions of tunability. Only systems with demonstrated broad regions of tunability are included here. (Many other systems which make use of rare gases and molecular gases have been reported, but have limited tunability (ref. 21).) The resulting tunable radiation retains all of the properties of the generating laser radiation including coherence, directionality, narrow linewidth and short-pulse duration, with the exception of high intensity. Nevertheless the generated VUV radiation has peak spectral brightness several orders of magnitude greater than that available from incoherent sources, including synchrotrons. Moreover, the monochromaticity achieved to date provides resolving powers $\lambda/\Delta\lambda > 10^5$, and thus these sources are ideally suited for high-resolution spectroscopy.

APPLICATIONS IN SPECTROSCOPY

To date, the laser-driven sources based on harmonic generation and frequency mixing have been used in a number of experiments to measure radiative lifetimes and to record absorption and laser-induced fluorescence spectra. While some of the anti-Stokes Raman sources have demonstrated high intensity and are being applied to specific problems of impurity detection in plasmas, their general utility in spectroscopy awaits the development of systems with broad tunability. Here, several typical spectroscopic applications of the above VUV and XUV sources are given to illustrate their usefulness.

The monochromaticity (∿0.2 cm^{-1}) and short pulse duration (∿1 to 5 ns) of these sources makes possible the measurement of radiative lifetimes of specific rovibronic levels. As an example, recent results (ref. 39) with CO are shown in Fig. 10. Initially, the fluorescence excitation spectrum of the (0,0) band of the transition $A^1\Pi \rightarrow X^1\Sigma$ was recorded (154 to 155.5 nm) with an effective resolution of ∿0.3 cm^{-1}. The observed lines were identified; then the exciting radiation was tuned to each rovibronic line and the decay of fluorescence intensity with time was measured. In this way, lifetimes for levels J' = 1 to 29 of the v' = 0 level were obtained from the decay rates for transitions in the P, Q, and R branches. The results indicate strong perturbations at J' = 9, 16, and 27, as shown by a doubling of lifetimes over those of unperturbed levels (τ_u ∿ 10 ns).

The electronic spectra of rare gas dimers have been a subject of interest for many years, mainly because these dimers are model systems for studying van der Waal's interactions, and because of their potential as media for VUV and XUV lasers. Yet very little is known about the excited states of these dimers. Two experimental techniques were combined in our laboratory for this investigation (ref. 40): four-wave sum-mixing (4-WSM) and a pulsed supersonic jet to produce rotationally and vibrationally cold dimer molecules. In this way it was possible to resolve rovibronic structures in several isotopic band systems of Xe_2, Kr_2 and Ar_2, in the region 150 to 104 nm. Thus, for the first time, the spectroscopic constants and potential energy curves of the lowest three excited states were determined for each of these dimers. With the spectrum shown in Fig. 11, it was possible to demonstrate that Hund's case (c) coupling holds for Ar_2, and to establish the symmetries of the electronic states.

In Fig. 12 is shown a portion of the 7-0 Lyman band of H_2 obtained by Marinero et al. (ref. 36) using the experimental arrangement given in Fig. 9. As shown by the lower trace taken at 1/10 the pressure of that for the absorption spectrum (upper trace), detection by laser-induced fluorescence is clearly a far more sensitive technique. The observation of this spectrum of H_2 at such low density ($\sim 2 \times 10^8$ molecules/cm^3) suggests the possibility of investigating the resonance Raman spectrum of H_2 in the near future. Obviously, H_2 would be an ideal medium for a complete understanding of the resonance Raman effect.

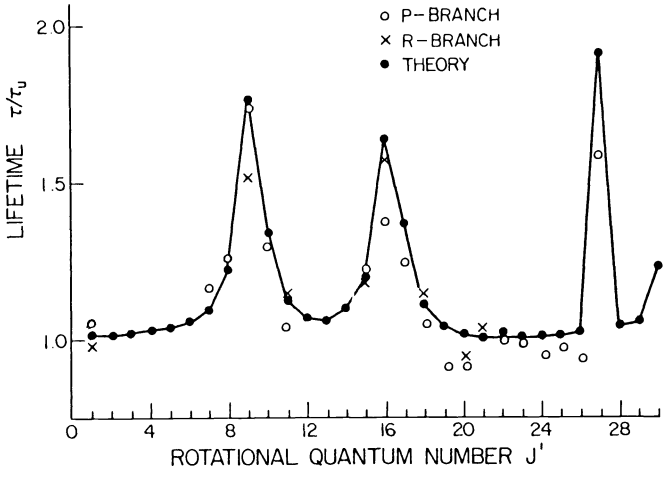

Fig. 10.
Radiative lifetimes (ref. 39) for rovibronic levels of the A $^1\Pi$(v' = 0) state of CO.

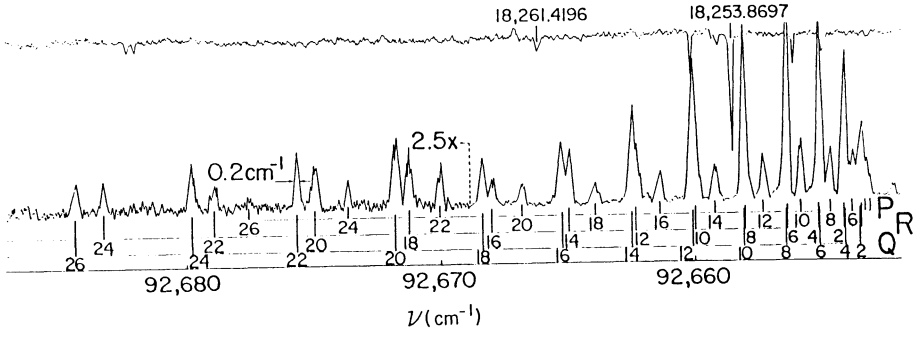

Fig. 11. Spectrum (ref. 40) of the 25-0 band (at 108 nm) for the $Al_u \leftarrow X\ 0_g^+$ transition in Ar_2, obtained at a resolving power of 5×10^5. Three rotational branches are resolved and identified, thus establishing Hund's coupling case (c) for Ar_2. (The uranium optogalvanic spectrum at the top was used for wavelength calibration.)

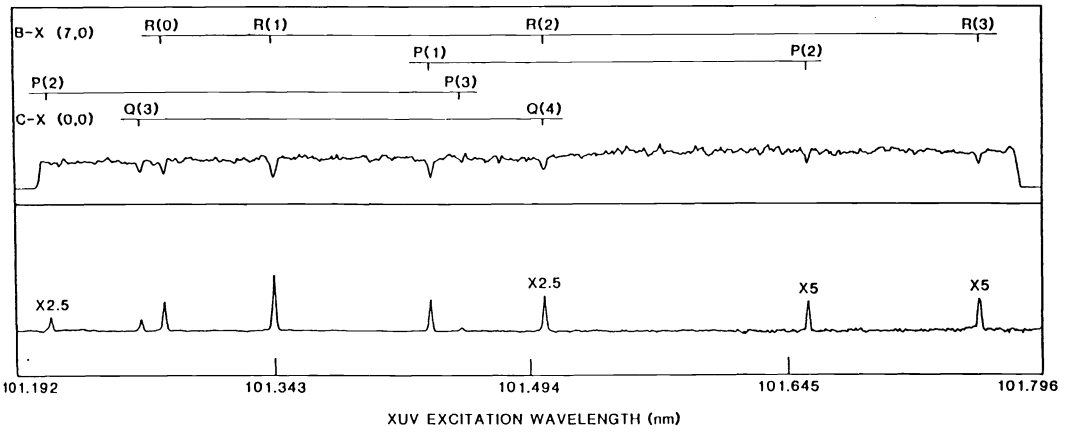

Fig. 12. H_2 absorption spectrum (ref. 36) at top (taken with a pressure of 5×10^{-5} Torr) and fluorescence excitation spectrum at bottom (4×10^{-6} Torr) in the region 101.2 - 101.8 nm.

REFERENCES

1. E.J. Woodbury and W.K. Ng, Proc. IRE, 50, 2347 (1962): G. Eckhardt, R.W. Hellwarth, F.J. McClung, S.E. Schwarz, D. Weiner, and E. J. Woodbury, Phys. Rev. Lett., 9, 455 (1962).
2. B.P. Stoicheff, in Proc. International School of Physics "Enrico Fermi", Course XXXI, 1963, C. H. Townes and P. A. Miles, eds., Academic Press, New York, pp. 306-325 (1964): B. P. Stoicheff, Phys. Lett. 7, 186 (1963).
3. R.W. Minck, R.W. Terhune, and W.G. Rado, Ap. Phys. Lett., 3, 181 (1963).
4. N. Bloembergen, Am. J. Phys., 35, 989 (1967): A. Penzkofer, A. Laubereau, and W. Kaiser, Prog. Quant. Electr., 6, 55 (1979). Y.R. Shen, The Principles of Nonlinear Optics, Wiley-Interscience, New York (1984).
5. T.R. Loree, R.C. Sze, and D.L. Barker, Appl. Phys. Lett., 31, 37 (1977); T.R. Loree, R.C. Sze, D.L. Barker, and P.B. Scott, IEEE J. Quantum Electron., QE-15, 337 (1979).
6. R.S. Hargrove and J.A. Paisner, in Topical Meeting on Excimer Lasers, Opt. Soc. Am. Washington, D.C. (1979), Paper ThA6.
7. V. Wilke and W. Schmidt, Appl. Phys., 16, 151 (1978); 18, 177 (1979).
8. H. Schomburg, H.F. Döbele, and B. Rückle, Appl. Phys., B30, 131 (1983).
9. H.F. Döbele, M. Röwekamp, and B. Rückle, IEEE J. Quantum Electron., QE-20, 1284 (1984).
10. M. Maeda and A. Takahashi, private communication (1986); A. Takahashi, M. Sumi, and M. Maeda, Opt. Commun., 55, 193 (1985).
11. W. Sasaki, Y. Ulhara, K. Kurosawa, E. Fugiwara, Y. Kato, and M. Yamanaka, Rev. Laser Engineering, 14, 370 (1986); Opt. Lett., 10, 487 (1985).
12. R.L. Carmen and W.H. Lowdermilk, Phys. Rev. Lett., 33, 190 (1974).
13. S.E. Harris, Ap. Phys. Lett., 31, 498 (1977): L.J. Zych, J. Lukasik, J.F. Young, and S.E. Harris, Phys. Rev. Lett., 40, 1493 (1978).
14. J.C. White and D. Henderson, Phys. Rev., A25, 1226 (1982): Opt. Lett., 7, 204 (1982): Opt. Lett., 8, 520 (1983): IEEE J. Quantum Electron, QE-20, 462 (1984).
15. J.C. White, Opt. Lett., 9, 38 (1984).
16. K. Ludewigt, H. Schmidt, R. Dierking, and B. Wellegehausen, Opt. Lett., 10, 606 (1985).
17. K. Ludewigt, K. Birman, and B. Wellegehausen, Appl. Phys., B33, 133 (1984): B. Wellegehausen, K. Ludewigt, and H. Welling, Proc. Soc. Photo-Opt. Instrum. Eng., 492, 10 (1985).
18. J.A. Armstrong, N. Bloembergen, J. Ducuing, and P.S. Pershan, Phys. Rev., 127, 1918 (1962).
19. R.T. Hodgson, P. P. Sorokin, and J.J. Wynne, Phys. Rev. Lett., 32, 343 (1974).
20. C.R. Vidal, Appl. Opt., 19, 3897 (1980).
21. W. Jamroz and B.P. Stoicheff, in Progress in Optics XX, E. Wolf ed., North-Holland, Amsterdam, 325 (1983).
22. G.H.C. New and J.F. Ward, Phys. Rev. Lett., 19, 556 (1967).
23. R.B. Miles and S.E. Harris, Appl. Phys. Lett., 19, 385 (1971).
24. K.D. Bonin and T.J. McIlrath, J. Opt. Soc. Am., B2, 527 (1985).
25. P.R. Herman and B.P. Stoicheff, Opt. Lett., 10, 502 (1985).
26. J. Bokor, P.H. Bucksbaum, and R.R. Freeman, Opt. Lett., 8, 217 (1983).
27. A.H. Kung, Opt. Lett., 8, 24 (1983).
28. P.R. Herman, P.E. LaRocque, R.H. Lipson, W. Jamroz, and B.P. Stoicheff, Can. J. Phys., 63, 1581 (1985).
29. A.H. Kung, J.F. Young, G.C. Bjorklund, and S.E. Harris, Phys. Rev. Lett., 29, 985 (1972): A.H. Kung, Appl. Phys. Lett., 25, 653 (1974).
30. R. Hilbig and R. Wallenstein, Appl. Opt., 21, 913 (1982); IEEE J. Quantum Electron., QE-17, 1566 (1981).
31. R. Hilbig and R. Wallenstein, Opt. Commun., 44, 283 (1983); R. Hilbig A. Lago, and R. Wallenstein, Opt. Commun., 49, 297 (1984); R. Hilbig, G. Hilber, A. Lago, B. Wolff and R. Wallenstein, Comments At. Mol. Phys., 18, 157 (1986).
32. J. Reintjes, C. Y. She, and R. C. Eckardt, IEEE J. Quantum Electron, QE-14, 581 (1978).
33. H. Egger, T. Srinivasan, K. Hohla, H. Scheingraber, C.R. Vidal, H. Pummer, and C.K. Rhodes, Appl. Phys. Lett., 39, 37 (1981); Opt. Lett., 5, 282 (1980).
34. D. Cotter, Opt. Commun., 31, 397 (1979).
35. F.J. Northrup, J.C. Polanyi, S.C. Wallace, and J.M. Williamson, Chem. Phys. Lett., 105, 34 (1984).
36. E.E. Marinero, C.T. Rettner, R.N. Zare, and A.H. Kung, Chem. Phys. Lett., 95, 486 (1983).
37. R. Mahon and F.S. Tomkins, IEEE J. Quantum Electron., QE-18, 913 (1982).
38. R.R. Freeman, R.M. Jopson, and J. Bokor, in Laser Techniques for Extreme Ultraviolet Spectroscopy, T.J. McIlrath and R.R. Freeman, eds., Amer.Inst. Phys., New York, 422 (1982).
39. A.C. Provorov, B.P. Stoicheff, and S.C. Wallace, J. Chem. Phys., 67, 5393 (1977); M. Maeda and B.P. Stoicheff, in Laser Techniques for Extreme Ultraviolet Spectroscopy, T.J. McIlrath and R.R. Freeman, eds., Amer. Inst. Phys., New York, 162 (1982).
40. P.R. Herman, A.A. Madej, and B.P. Stoicheff, Chem. Phys. Lett. (in press); R.H. Lipson, P.E. LaRocque, and B.P. Stoicheff, J. Chem. Phys., 82, 4470 (1985); P.E. LaRocque, R.H. Lipson, P.R. Herman, and B.P. Stoicheff, J. Chem. Phys., 84, 6627 (1986).